STRUCTURAL BIOLOGY

Volume 74 (2018)

Supporting information for article:

Membrane protein crystals for neutron diffraction

Thomas Lykke-Møller Sørensen, Samuel John Hjorth-Jensen, Esko Oksanen, Jacob Lauwring Andersen, Claus Olesen, Jesper Vuust Moller and Poul Nissen

Table S1 Favourable membrane protein cases suitable for NMX

PDB	Protein	Resolution (Å)	Space group	a, b, c (Å)	α, β, γ (°)	Reference
4BVM	Human myelin peripheral membrane protein P2	0.93	P 4_1 2_1 2	58.07, 58.07, 101.50	90.00, 90.00, 90.00	(Laulumaa *et al.*, 2015)
5JAE	$LeuT_{Aa}$ leucine transporter	1.65	P 2_1	81.57, 92.08, 92.47	90.00, 95.18, 90.00	(Yamashita *et al.*, 2005)
4US3	MhsT multi-hydrolphobic amino acid transporter	2.1	P 2	44.28, 49.89, 110.05	90.00, 96.76, 90.00	(Malinauskaite *et al.*, 2014)
4AV3	Na^+-translocating M-PPase with metal ions in active site	2.6	P 2_1	83.52, 107.78, 102.52	90.00, 108.50, 90.00	(Kellosalo *et al.*, 2012)
5NG9	Glutamate receptor 2	1.15	P 2_1 2_1 2	62.22, 88.14, 47.96	90.00, 90.00, 90.00	(Mollerud *et al.*, 2017)
2W2E	Aqy1 yeast aquaporin (pH 3.5)	1.15	I 4	91.45, 91.45, 80.82	90.00, 90.00, 90.00	(Fischer *et al.*, 2009)
2NTU	Bacteriorhodopsin	1.53	P 6_3	60.97, 60.97, 110.39	90.00, 90.00, 120.00	(Lanyi & Schobert, 2007)
3HB3	Cytochrome C Oxidase	2.25	P 2_1 2_1 2_1	83.40, 150.47, 157.19	90.00, 90.00, 90.00	(Koepke *et al.*, 2009)
2J8C	Photosynthetic Reaction Center	1.9	P 3_1 2 1	138.69, 138.69, 184.61	90.00, 90.00, 120.00	(Koepke *et al.*, 2007)
3C1J	AmtB (ammonia channel)	2.0	P6_3	110.23, 110.23, 84.64	90.00, 90.00, 120.00	(Javelle *et al.*, 2008)

5WIU	Dopamine D_4 receptor complexed with nemonapride	2.0	C 2 2 2_1	67.69, 164.05, 84.13	90.00, 90.00, 90.00	(Wang *et al.*, 2017)
6EU6	Sensor Amt Protein	2.0	P 6_3	99.75, 99.75, 89.07	90.00, 90.00, 120.00	(Pfluger *et al.*, 2018)
4RYQ	Translocator Protein (TSPO), apo type 2 monomer	1.7	P 2_1 2_1 2_1	28.71, 54.62, 106.91	90.00, 90.00, 90.00	(Guo *et al.*, 2015)
3TDO	FNT3 Hydrosulphide Channel (HSC), pH 9.0	2.2	P 2_1 2_1 2_1	98.82, 118.74, 149.82	90.00, 90.00, 90.00	(Czyzewski & Wang, 2012)

Table S2 Favourable SERCA crystal forms for NMX

PDB	Crystal Form	Resolution (Å)	Space group	a, b, c (Å)	α, β, γ (°)	Ligands	Reference
1T5S	Ca2E1•AMPPCP	2.6	C 1 2 1	162.44, 76.26, 151.16	90.00, 108.70, 90.00	AMPPCP, Ca2+, K+, Mg2+	(Sorensen *et al.*, 2004)
1XPS	E2(TG)•AlF4-	3.0	P 2_1 2_1 2_1	86.51, 119.27, 142.26	90.00, 90.00, 90.00	Thapsigargin, AlF4, K+, Mg2+	(Olesen *et al.*, 2004)
1T5T	Ca2E1•AlF4-•ADP	2.9	C 1 2 1	162.48, 75.62, 151.65	90.00, 108.82, 90.00	ADP, AlF4, Ca2+, K+, Mg2+	(Sorensen *et al.*, 2004)
2C9M	Ca2E1	3.0	P 1	64.95, 81.28, 131.01	97.64, 99.94, 95.22	Ca2+, K+, Cl-	(Jensen *et al.*, 2006)
2O9J	E2(CPA)•MgF4 2-	2.65	C 1 2 1	175.38, 69.88, 143.41	90.00, 107.10, 90.00	CPA, MgF4-, Mg2+, Na+	(Moncoq *et al.*, 2007)
2OA0	E2(CPA)•ADP	3.4	P 1 2_1 1	62.50, 96.84, 154.86	90.00, 94.83, 90.00	ADP, CPA, Mg2+	(Moncoq *et al.*, 2007)
2EAR	E2(TG)	3.1	P 1 2_1 1	62.85, 95.94, 154.49	90.00, 94.90, 90.00	Thapsigargin	(Takahashi *et al.*, 2007)
2EAT	E2(TG+CPA)	2.9	P 1 2_1 1	62.90, 95.64, 155.10	90.00, 95.24, 90.00	Thapsigargin, CPA	(Takahashi *et al.*, 2007)
2ZBF	E2(TG)•BeF3-	2.4	P 2_1 2_1 2_1	90.52, 136.47, 106.62	90.00, 90.00, 90.00	Thapsigargin, BeF3-, Mg2+	(Toyoshima *et al.*, 2007)
2ZBG	E2(TG)•AlF4-	2.55	C 1 2 1	117.50, 70.20, 143.40	90.00, 106.80, 90.00	Thapsigargin, AlF4-, Mg2+	(Toyoshima *et al.*, 2007)

3B9R	E2(TG)•AlF4--AMPPCP	3.0	P 1 2_1 1	131.98, 94.43, 136.18	90.00, 107.79, 90.00	AMPPCP, AlF4-, K+, Mg2+	(Olesen *et al.*, 2007)
3BA6	Ca2E1~P•AMPPN	2.8	C 1 2 1	162.51, 75.97, 152.41	90.00, 109.01, 90.00	AMP Phosphoramidate, Ca2+, K+	(Olesen *et al.*, 2007)
3FPB 2O9J	E2(CPA)•MgF42-•ATP	2.55	C 1 2 1	175.36, 69.87, 143.50	90.00, 107.16, 90.00	ATP, CPA, MgF42-, K+, Mg2+	(Laursen *et al.*, 2009)
3FPS 2OA0	E2(CPA)•ADP	3.2	P 1 2_1 1	62.34, 96.50, 155.13	90.00, 94.84, 90.00	ADP, CPA, Mg2+	(Laursen *et al.*, 2009)
3AR8	E2(TG)•AlF4-•TNP-AMP	2.6	C 1 2 1	176.86, 69.87, 141.81	90.00, 106.71, 90.00	Thapsigargin, TNP-AMP, AlF4-, Mg2+, Na+	(Toyoshima *et al.*, 2011)
3AR9	E2(TG)-BeF3-•TNP-AMP	2.6	P 2_1 2_1 2	90.39, 135.81, 105.43	90.00, 90.00, 90.00	Thapsigargin, TNP-AMP, BeF3-, Mg2+, Na+	(Toyoshima *et al.*, 2011)
4YCL	E2(CPA)	3.25	P 1 2_1 1	63.04, 96.03, 155.42	90.00, 95.09, 90.00	CPA, K+, Mg2+	(Takahashi *et al.*, 2007)
5A3Q	E2(TG)•VO3-•TNP-AMPPCP	3.05	P 2_1 2_1 2	86.43, 118.78, 141.83	90.00, 90.00, 90.00	TNP-AMPPCP, Thapsigargin,vanadium, K+, Cl-, Mg2+	(Clausen *et al.*, 2016)
5A3S	E2(TG)•VO3-•TNP-ATP	3.3	P 1 2_1 1	130.56, 93.78, 135.69	90.00, 107.26, 90.00	TNP-ATP, Thapsigargin,vanadium, K+, Cl-, Mg2+	(Clausen *et al.*, 2016)
5XA7	Ca2E1	3.2	C 1 2 1	166.20, 64.54, 146.22	90.00, 98.12, 90.00	1,2-dioleoyl-SN-glycero-3-phosphocholine, Ca2+, Na+	(Norimatsu *et al.*, 2017)
5XA8	Ca2E1•AlF4-•ADP	3.2	C 1 2 1	162.97, 75.02, 152.24	90.00, 109.31, 90.00	1,2-dioleoyl-SN-glycero-3-phosphocholine,	(Norimatsu *et al.*, 2017)

ADP, AlF4-,Ca2+,
Mg2+

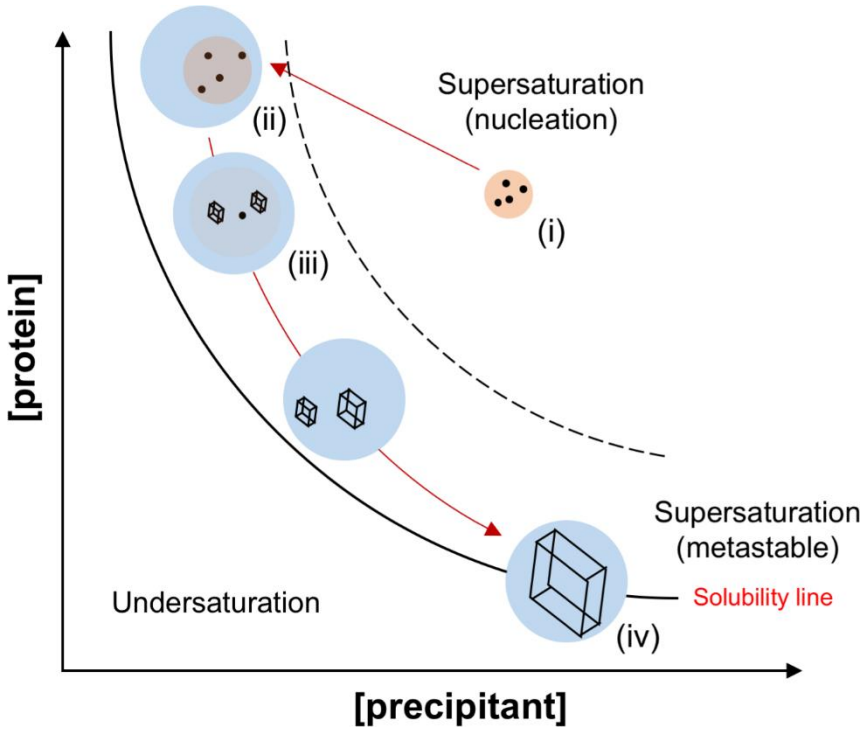

Figure S1 Decoupling nucleation and growth phases. Nucleation (**i**) occurs at typical (< 5 µL) drop volumes over a period of ~24 hours (before crystals develop beyond infancy). A high volume of protein-rich solution is added to the initial drop, bringing the combined conditions into the ↑ [protein] / ↓ [precipitant] area of the metastable zone (**ii**). Protein concentration drops as a few nuclei survive to become fully-fledged crystals and the mother liquor proceeds towards the solubility line (**iii**). Careful selection of reservoir composition and volume keeps the mother liquid in the metastable phase – counteracting the loss of [protein] due to crystal growth by increasing [precipitant] *via* vapour diffusion – and results in crystals of maximal size when the solubility line is reached (**iv**). As crystal growth occurs along a smooth and uninterrupted phase-time pathway, diffraction quality should be maximised.

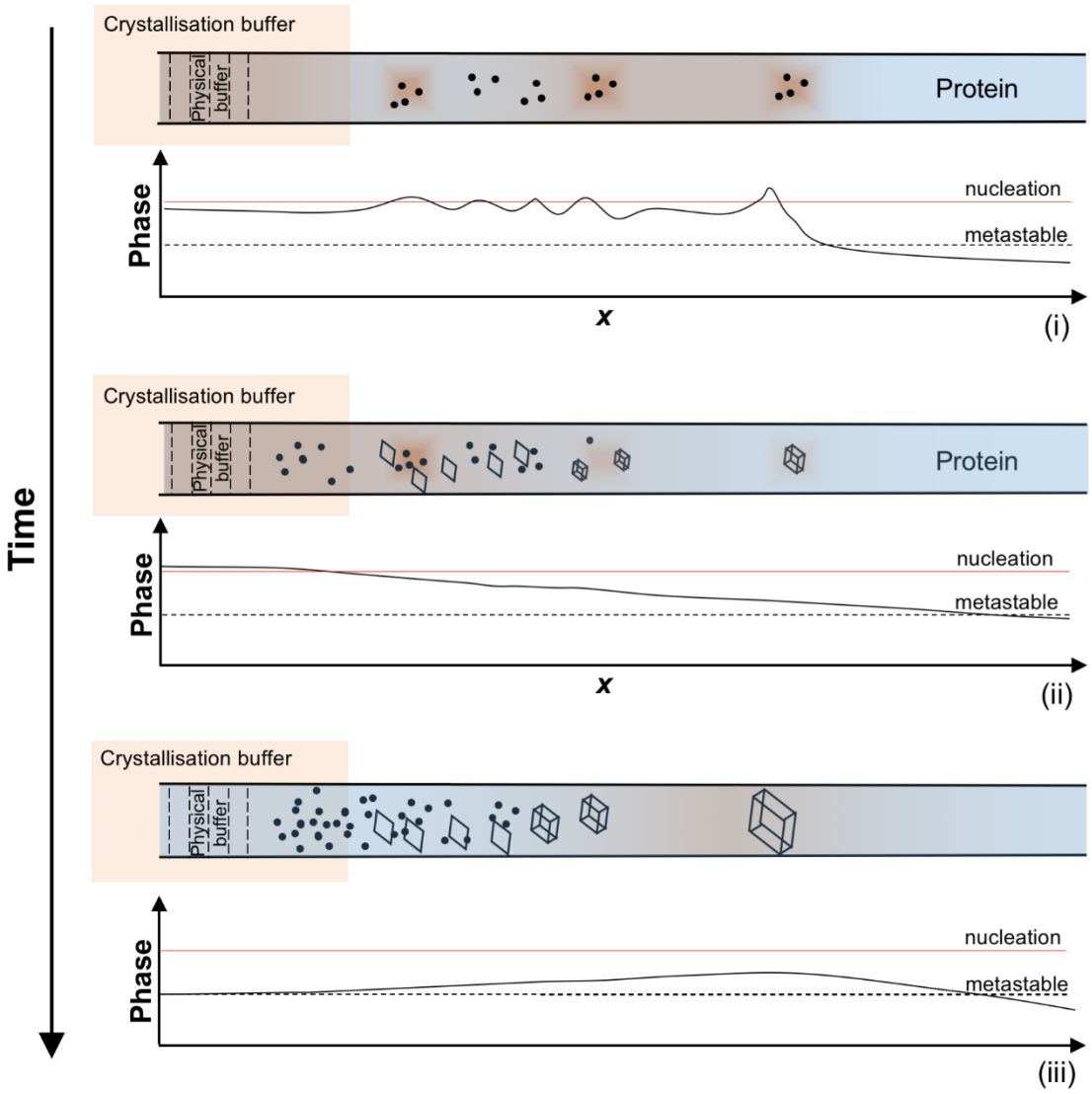

Figure S2 Dynamics of counter-diffusion crystallisation. Initially, a supersaturation wave moves along the capillary, sporadically crossing the nucleation threshold and forming nuclei (**i**). Afterwards, a more stable [precipitant] gradient combines with the remaining pockets of high (and varying) supersaturation, and nuclei develop into a mixture of crystal polymorphs and precipitates (**ii**). This gradient slowly moves through the capillary, counteracting the drive towards the solubility line as protein leaves the solution as precipitate or crystal growth (**iii**). Excessive [precipitant] near the physical buffer forces all excess protein to drop out as precipitate, and the mother liquor reaches the solubility limit. Further along the capillary, [precipitant] is more optimal, keeping the mother liquor within the metastable (growth) zone and resulting in large crystals. The red/orange colour inside capillaries indicates that various amounts of protein precipitation is normally observed.

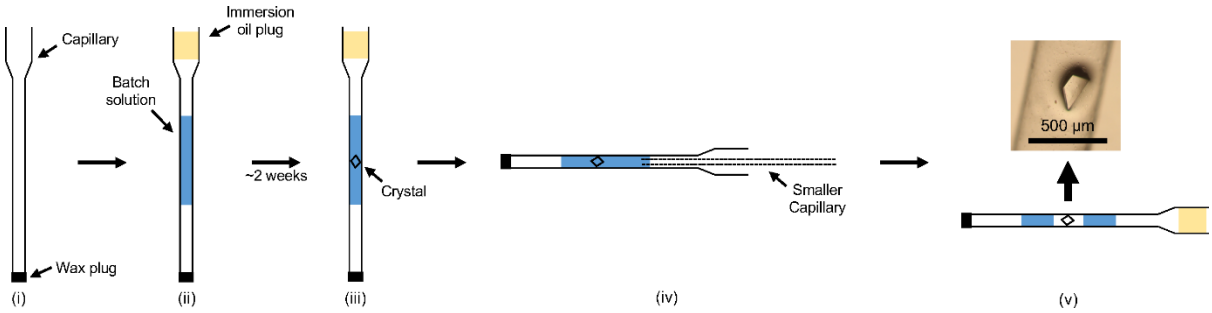

Figure S3 Mounting single SERCA crystals in capillary. Capillary bottoms were first sealed with wax (**i**), before batch solution was injected into the middle of the capillary – leaving an air gap above and below the batch solution – and the capillary top was sealed with immersion oil (**ii**). After a period of ~2 weeks, a few single crystals developed within the batch solution (**iii**). A suitable crystal was selected, the immersion oil plug removed, and a smaller capillary was inserted into the crystal-containing capillary (**iv**). This smaller capillary was used to suck out the mother liquor surrounding the crystal, after which it was removed and the crystal-containing capillary re-sealed with immersion oil (**v**). The isolated crystal was now ready to be mounted directly onto the X-ray goniometer for diffraction studies.

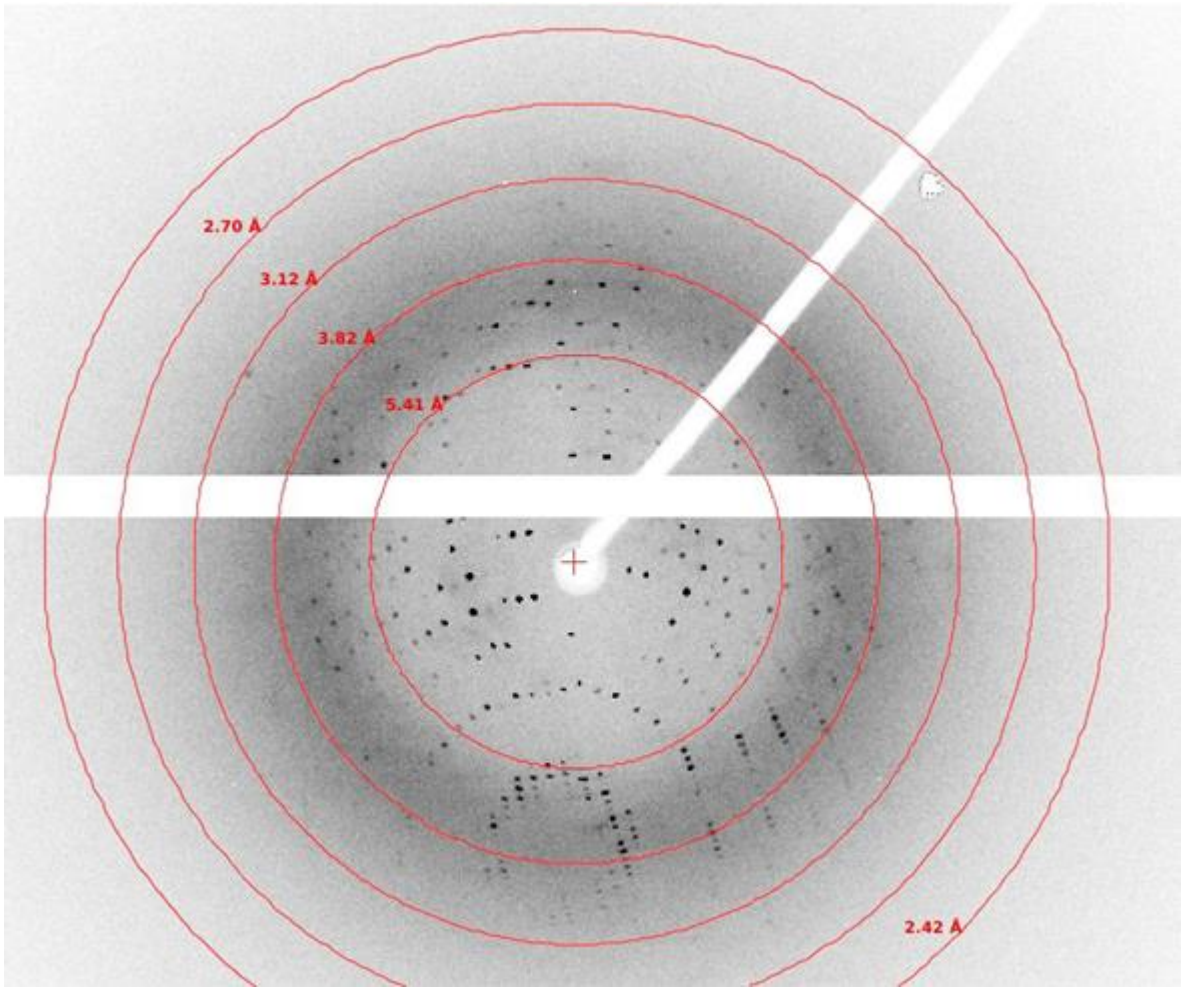

Figure S4 Diffraction image. The maximum diffraction of the tested Ca_2E1-AMPPCP crystals was ~3.0 Å. The frame shown is of an initial test shot of comprising a 0.5 ° rotation over a 35 s exposure.

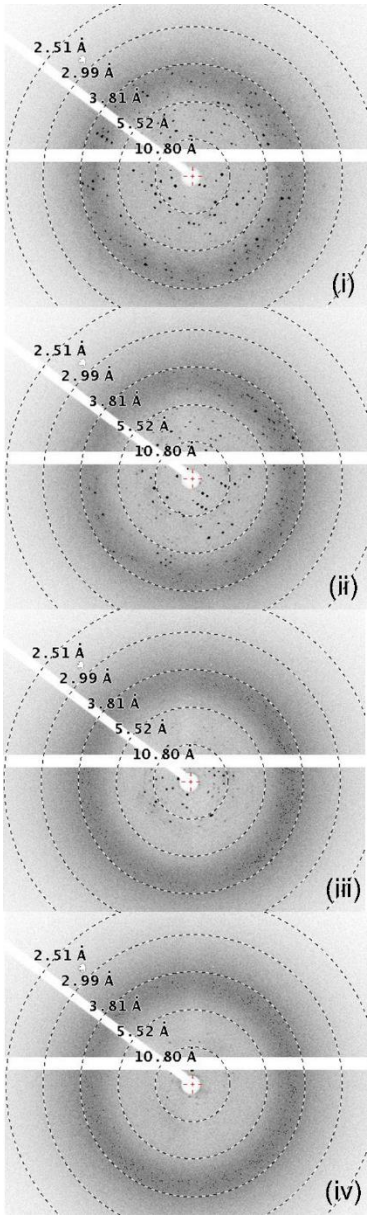

Figure S5 Examples of radiation sensitivity. Images **i – iv** (corresponding to frames 1, 60, 120, and 180 respectively) show the loss of diffraction quality over time. Each frame comprised of a 0.5 ° rotation over a 35 s exposure, meaning maximum resolution deteriorated from ~3.5 Å (**i**) to ~8 Å (**iii**) over a time period of only 70 mins.

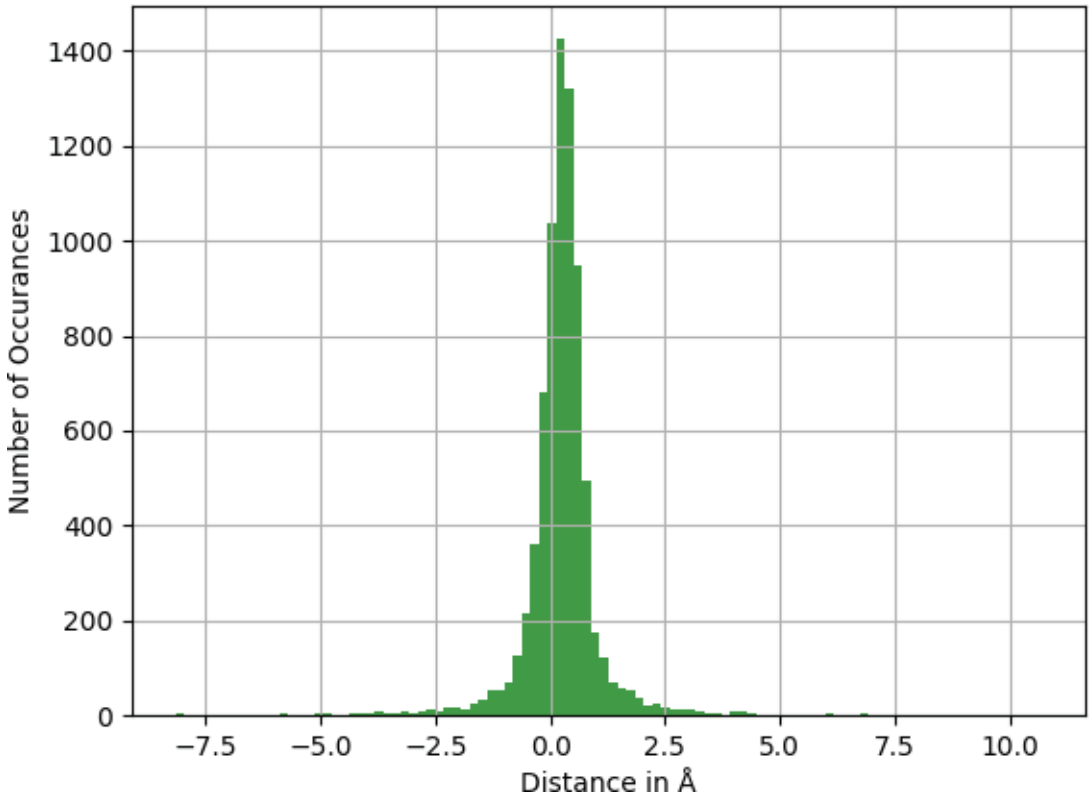

Figure S6 Temperature-dependent perturbation of the SERCA1 structure. The distances from each atom in the structures to the protein centre-of-mass is compared for the RT (6hef) and cryo (3n8g) structures. The histogram shows the distribution of the differences in distance for equivalent atoms in the two structures (mean=0.26, SD=0.91).